RSC Advances

ROYAL SOCIETY OF CHEMISTRY

www.rsc.org/advances

Cite this: DOI: 10.1039/c0xx00000x

www.rsc.org/xxxxxx

ARTICLE TYPE

Improving the SERS Detection Sensitivity on Aromatic Molecules by PDMS Coated Au Nanoparticles Monolayer Film

Chen Qian‡, Qinghua Guo‡, Minmin Xu, Yaxian Yuan* and Jianlin Yao*'

Received (in XXX, XXX) Xth XXXXXXXXX 20XX, Accepted Xth XXXXXXXXX 20XX

DOI: 10.1039/b000000x

Surface enhanced Raman spectroscopy (SERS) has been considered as a promising tool for detecting the targets with single molecule sensitivity. However, the SERS detection on targets without specific adsorption group is still remained a significant challenge. In this paper, we reported a facile strategy to fabricate PDMS film coated Au nanoparticles monolayer film (Au MLF) composite substrate for improving SERS detection on aromatic molecules in water and atmospheres. The toluene, benzene and nitrobenzene were used as the targets to evaluate the performance of the composite substrates. The results indicated PDMS film played the vital role to capture and preconcentrate these targets for improving the capability in SERS detection of these targets. The performance was critically dependent on the hydrophobicity, functional group and the permeability of the targets. This composite substrate was favorable for the toluene and nitrobenzene rather than the benzene. The limit of detection (LOD) for toluene and nitrobenzene was decreased about two orders of magnitude on PDMS-Au MLF by comparing to that on naked Au MLF, while one order of magnitude for benzene. It was estimated to be 0.5 ppm, 0.6 ppm and 78 ppm for toluene, nitrobenzene and benzene, respectively. The results demonstrated that this approach could be developed as a promising tool to detect numerous targets which were non-specifically adsorbed onto the metallic nanostructures. It opened a window towards the general application of SERS for in situ monitoring pollutants in water and atmospheres.

Introduction

Various volatile organic compounds (VOCs) and semivolatile organic compounds (SVOCs), involving benzene, toluene, nitrobenzene and their derivative, are considered to be carcinogenic, mutagenic, and have significant harmful effects on human health and environmental security. [1-3] The typical identification techniques were mainly relied on the expensive instrumentation, such as gas chromatography (GC), gas chromatography-mass spectrometry (GC-MS), and high performance liquid chromatography (HPLC). Although these techniques held the acceptable sensitivity and stability, the involved preparation process and subsequent analytical procedure were still complex and time-consuming. [4] Moreover, they were completely laboratory based, and lacked the instantaneous and in situ monitoring capability, particularly for the remote identification and monitoring. Therefore, with the increasing diffusion and accumulation of the pollutant to the environments in water and atmosphere, the development of in situ technologies is highly desired for the rapid identification.

Surface enhanced Raman spectroscopy (SERS) has been attracted considerable attention for the chemical sensing, environmental monitoring and other relevant fields. With the sensitivity up to single molecule level and the capability in identification molecules through the vibrational fingerprint, it is considered as a promising tool for the detection of trace molecules under ambient conditions, including liquids, atmosphere, tissue and so on.[5-8] Moreover, the compact integration of modern Raman spectrometer has improved the performance for portable and remote monitoring.[9] Generally, the strong SERS effect was mainly contributed by the electromagnetic and charge transfer enhancements. For the former, the generation of surface plasmon resonance (SPR) from the appropriate nanostructures induced the localized electric field to enhance the Raman signal of molecules which was located in a certain distance (nano/subnanometer scale) away from the surface. For the latter, it was originated from the excitation photon driven charge transfer between the metal and the molecules which were immobilized at metal surface. Therefore, it was essential to locate the targets near the enhancement source (SERS substrates). Generally, the probes attached with specific groups, involving thio, amino, nitrile, etc., were allowed to immobilize to the metal surface directly for providing the strong SERS signal, i.e. decreasing the limit of detection (LOD). [10-12] Therefore, the generalities on targets for SERS detection still remained a significant challenge, particularly for the analytes without specific adsorption group, such as aromatic molecules.

Since the aromatic compounds, such as benzene, toluene, contained no specific functional group and held a low affinity toward the metallic plasmonic surface, it was really difficult to detect them directly by SERS. In order to overcome this drawback, various techniques have been developed to immobilize

these targets onto the substrate to increase the sensitivity, i.e. locating the targets at the zone of the electromagnetic field.[13]Among them, as a general strategy, different kinds of materials were modified onto the substrates, which allowed the sufficient weak adsorbed targets to be immobilized near the plasmonic nanostructures through the interaction between the modified functional layer and the targets. [13-31] For example, based on host-guest molecular recognition, the targets were selectively trapped through the host-guest interactions resulting in the preconcentration of targets. For molecules lacking the affinity to metallic surface, the particular construction of host molecules has cavities to specifically trap targets to be close to the SERS substrates.[14-17]In other cases, self-assembly monolayers of thiol and alkylsilane on SERS substrates made the metal surface to be hydrophobic to allowed the inclusion of the targets into the zone of electromagnetic enhancement, i.e. immobilization of the targets in the range of the long distance of electromagnetic enahncement.[18-20] The noble metal modified magnetic nanoparticles provided the alternative preconcentration of targets by an external magnetic field. Moreover, the magnetic field induced the aggregation of nanocomposite to generate numerous plasmonic "hot spots", thus improving the LOD of targets without the specific group to anchor to the metal surface.[21-23]Similarly, the metal-organic frameworks (MOFs) were successfully modified to the plasmonic nanostructures and played as the host to capture the weak adsorbed targets through their unique porous structures of MOFs, particularly for the gas targets in atmospheres. A few of these reports demonstrated the nature of MOFs made it become the very promising composite substrate for the preconcentration of weak adsorbed molecules to be close to the metal surface. [24-27] The metallized polymers such as Au/Ag nanoparticle-polydimethylsiloxane (PDMS) nanocomposites exhibited unique immobilization capability for the SERS detection of aromatic compounds [28-31]. However, it was mainly used to capture targets with functional groups, such as nitro, hydrocarboxyl, and hydroxyl, to improve the SERS sensitivity. [31]To our best knowledge, there is no reports on the SERS detection of aromatic molecules, such as benzene, toluene, ethyl benzene and xylene by combining the PDMS film and metallic plasmonic nanostructures. Actually, the PDMS incorporated with Au nanoparticles exhibited the extremely high swelling capability (larger than six times). Thus, it has been already explored to capture the aromatic molecules both in water and atmospheres, i.e. cleaning up the environments. Moreover, the composite could be regenerated simply by heating to about 300 °C in air. [32] Due to the strong adsorption capability, PDMS was also used as a sorbent for the detection of benzene, toluene, ethylbenzene and xylene in water and air by solid-phase extraction. [33-35] Therefore, it is certainly worth exploring the combination of PDMS and plasmonic nanostructures to detect the aromatic molecules without specific affinity groups. In this paper, the spin coating was explored to optimize the PDMA layer on the Au nanoparticles monolayer film (Au MLF). The layer thickness of PDMS was then tuned to achieve the maximum SERS enhancement by changing the concentration of PDMS solution. For such kind of composite, the inner layer of Au MLF generated the gigantic SERS effect, while the outer layer of PDMS played the vital role in capturing the aromatic targets. A series of aromatic molecules, involving the benzene, toluene and nitrobenzene, was served as the model system to demonstrate the capability of composite both for capturing the targets from water or atmosphere and SERS monitoring. This strategy provided an alternative approach to improve the SERS detection sensitivity of weak adsorbed targets and then extended the generality of SERS for different kinds of analytes.

Experimental Section

General

SYLGARD silicone elastomer base and SYLGARD 184 silicone elastomer curing agent were bought from Dow Corning Company. Polyvinylpyrrolidone was purchased from Acros. Chloroauric acid tetrahydrate ($HAuCl_4 \cdot 4H_2O$), hydroxylamine hydrochloride ($NH_2OH \cdot HCl$), trisodium-citrate, sulfuric acid (H_2SO_4, 95%-98%), hydrogen peroxide(H_2O_2,30%), toluene, benzene, nitrobenzene, tetrahydrofura (THF), acetone, ethanol were of analytical grade and purchased from Sinopharm Chemical reagent corporation. All aqueous solutions were prepared with Milli-Q water (≥18.2 MΩ·cm).

Characterizations

Scanning electron microscopy (SEM) images were taken using FEI QUANTA 200F. Raman spectroscopy was performed by using LabRam HR800 micro-Raman system (HR800, Horiba, Jobin Yvon,) with 632.8 nm laser excitation from a He-Ne laser. A 50× objective lens with working distance of about 8 mm was attached onto the Raman microscopy. The slit width and confocal pinhole were 100 μm and 400 μm, respectively. The laser power was about 5 mW on the surface.

Fabrication of SERS composite substrate

Preparation of Au nanoparticles by seeds growth method

According to classic Frens' approach, chloroauric acid tetrahydrate was reduced by trisodium-citrate to obtain Au nanoparticles with tunable diameter. [36] Typically, 100 mL 0.01% (w/v%) $HAuCl_4 \cdot 4H_2O$ solution was heated to boiling under vigorous stirring and then 2mL 1% (w/v%) trisodium-citrate was quickly added. After the color of the solution remained unchanged, the solution was heated for another 15 minutes with reflux condensation and then cooled down to the room temperature. The obtained Au nanoparticles with the mean diameter of 15 nm were served as the seeds. After that, the seeds solution of 25 mL, 1 mL 1% (w/v) PVP, 1 mL 1%(w/v) trisodium citrate, and 20 mL 25 mM hydroxylamine hydrochloride were mixed under room temperature, following with the addition of 20 mL 0.1% (w/v) chloroauric acid tetrahydrate drop by drop under stirring for 1 hour. The final Au nanoparticles were stable in the solution with the diameter of about 30 nm.

Preparation and transfer of Au MLF

Transferring a certain amount of the Au nanoparticles solution as prepared into a lab made evaporating system, then heated to 40 °C under the vacuum drying oven for about 16 hours. A compact packaged Au MLF was formed at the solution/air interface. Then the Au nanoparticles monolayer

film was transferred to clean silicon wafers as plasmonic nanostructures. The detail procedure for the formation of monolayer was given elsewhere. [37]

Coating PDMS layer to Au MLF

Silicone elastomer base and curing agent were mixed together by the ratio of 10:1 (in wt%) , and kept shaking for 1 hour followed with 20 min degassing in vacuum. The PDMS elastomer was diluted in tetrahydrofuran (THF) solution to obtain the concentration range from of 0.078% to 50%. In our case, the thickness of PDMS layer was controllable by changing the concentration of PDMS elastomer. 5 µl PDMS elastomer solution was dropped onto the Au MLF, and the spin coating procedure was accomplished after 600 s at the spin speed of 1000 rpm with the acceleration of 500 rpm·s^{-1}. Finally, the coated films on an Au MLFs were subsequently cured in a vacuum oven at 80 °C for about 6 h. [38]

SERS detection of aromatic molecules

Firstly, the PDMS-Au MLF composite substrate were rinsed by Milli-Q water three times. Secondly, 100 µl of target solution was dropped onto the substrate. Finally, the substrate contained target solution was moved to the microscopy attached to Raman spectrometer for recording the surface Raman spectra. The detection on the gas of target was carried out in a simulation of polluted atmospheric environment. Typically, 2µl pure liquid of target was dropped on a slide located 5 cm distance away from the PDMS-Au MLF composite substrate, and the recorded the time dependent SERS spectra until the achievement to the maximum band intensity. As a control, the same experiments were performed on the naked Au MLF under the same conditions.

Results and discussion

Screening the PDMS film thickness

It was well known that PDMS exhibited the high swelling ability for the preconcentration of the trace aromatic molecules, and it was already explored to remove the benzene, toluene and oil spills from polluted water.[33-35] In our present case, in order to achieve high sensitivity of SERS detection, three issues should be taken into account, i) the enhancement effect of the plasmonic nanostructures; ii) the numbers of target molecules located at the zone of electromagnetic field; and iii) the propagation of laser and the Raman signal though the PDMS film. For the first issue, the Au MLF was severed as the SPR source, which contributed the strong coupling effect between the adjacent nanoparticles. For the last two issues, the thickness of PDMS film became the critical factor on the performance of the substrate. The thicker PDMS film was beneficial for inhibiting the diffusion of targets to air, i.e. immobilizing more targets around the surfaces. However, it blocked the propagation laser and Raman signal, resulting in the notable decrease of SERS signal. Therefore, it was necessary to screen the favorable thickness of PDMS film. The previous studies indicated that the thickness of PDMS film was critically depended on spin duration, spin speed, and the concentrations of PDMS base material. To some extent, longer spin duration, faster spin speed and the lower concentrations of PDMS base attributed the thinner PDMS film. However, the thickness of PDMS layer can't be controlled by varying the spin speed and spin time to achieve a layer thickness under 5 µm.[39] As the thinner PDMS layers with the accurately controllable thickness have been fabricated by diluting PDMS base material in some organic solvents, such as hexane, tertbutyl alcohol, n-octane, and tetrahydrofuran (THF). [38-40]In our case, the THF was used to dilute uncured PDMS base materials. The SERS detection capability of the PDMS-Au MLF composite was evaluated by using toluene as target analyte. Figure 1 presented the typical morphology of the composite. It indicated that the Au MLF was well dispersed on Si wafer, and Au nanoparticles together with the interparticle spacing were discriminated unambiguously on the naked Au MLF With the increase of the concentration of PDMS base material, the surface of Au MLF was gradually covered. The interparticle spacing disappeared completely by using the pure PDMS base as coating solution (Figure 1 b-c).

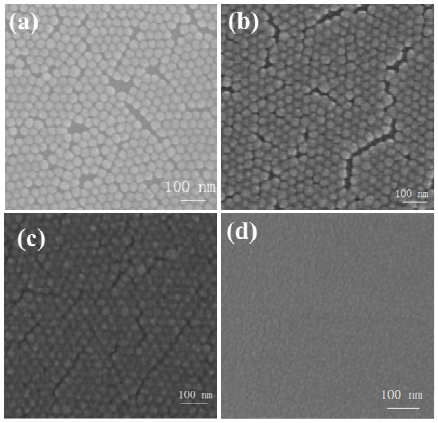

Figure 1 SEM images of naked Au MLF (a), and coated with PDMS by using different concentrations of PDMS base materials, 1.25% (b), 5% (c) and 100% (d).

The corresponding PDMS concentrations dependent SERS spectra of toluene were illustrated in Figure 2 as well as the concentration intensity of the band at 1003 cm^{-1}. It should be pointed out the spectral features observed from the composite substrate remained unchanged, indicating the same adsorption configuration of toluene on the composite substrate. It could be observed that the SERS intensity of band at 1003 cm^{-1} was dependent on the concentration of PDMS base material. In the diluted solution, it increased with the concentration, and reached the maximum at the concentration of about 1.25%. Then, it decreased remarkably as the concentration increased, and completely disappeared by using pure PDMS base material as the coating solution. It was reasonable to assume that the thickness of the PDMS exhibited the tendency to be thinner as decreasing concentrations of PDMS.[39] The present experimental facts demonstrated that the thinner PDMS film resulted in the difficulties for trapping the targets which contributed the weak SERS signal, while the thicker film decreased the propagation of laser and Raman signal to block the SERS signal dramatically. As a consequence, an appropriate thickness of the PDMS was essential both for trapping the targets and reducing the

attenuation of laser power and Raman signal. Based on the above experimental fact, the 1.25% PDMS base material in THF was used to fabricate the coating film. Based on the measurement by the spectroscopic ellipsometry and AFM, the favorable PDMS thickness of the composite substrate was ranging from 129 to 139 nm.

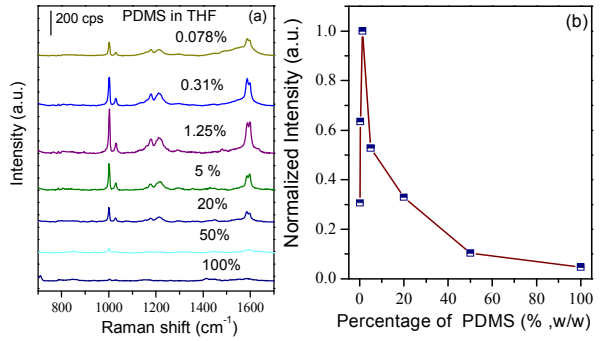

Figure 2 SERS spectra of the toluene on composite substrate. The PDMS was spin coated by the initial solution with different concentration of 100%, 50%, 20%, 5%, 1.25%, 0.31% and 0.078%, respectively (a). Profile of concentration-SERS intensity of band at 1003 cm^{-1} of 5 mM toluene solution (b).

Detection of toluene in water

Generally, the solubility of toluene was quite low in water, the saturation aqueous solution was about 7mM.[15] Figure 3 presented a serial of Raman and SERS spectra of toluene in water on different substrates. Major bands at 786 cm^{-1},1004 cm^{-1},1031 cm^{-1}, 1210 cm^{-1} and 1604 cm^{-1} were observed in the normal Raman spectra of pure toluene liquid (Figure 3a), which were assigned to the C-C bending, ring breathing mode, C-C stretching, ring-CH_3 stretching and ring-relevant modes[41-42]. The bands at 1003 cm^{-1} and 1030 cm^{-1} were dominated in the SERS spectrum, which were well matched the corresponding bands of toluene liquid (Figure 3e and a). It indicated the occurrence of physical interaction between the Au MLF and toluene, and the toluene was trapped by the PDMS film. The unexpected change was also observed from the bands at 786 cm^{-1} and 1604 cm^{-1}, i.e. the disappearance of former and significant enhancement of the latter together with a slight red-shift in frequency. It was mainly due to the surface selection rule for the enhancement effect. The background signal was negligible on the PDMS-Au MLF without adsorption of toluene (Figure 3d), and it should be noted that no Raman signal was observed from the toluene adsorbed on the PDMS coated Si wafer, indicating no plasmon enhancements from PDMS film (as shown in Figure 3b). Therefore, the observed SERS signal was originated from the toluene located at the long distance zone of electromagnetic enhancement.

As a comparison, the SERS spectrum of toluene adsorbed onto a naked Au MLF substrate was presented as Figure 3c. The similar spectral features of SERS from Au MLF with/without PDMS indicated the same interaction between toluene and substrate. However, the remarkable difference (about one order of magnitude) in the SERS intensity was mainly contributed by the increase of efficient targets around the composite substrate. Normally, on the naked Au MLF surface, the polyvinylpyrrolidone (PVP), which was added in preparation of Au nanoparticles, played the important role in improving the chemical selectivity and weakly affected the adsorption of toluene molecules, due to its hydrogen-bonding properties.[43] The PDMS film exhibited the similar function for trapping the targets. Mark and his coworkers estimated the diffusion and partition coefficient, and permeability of aromatic molecules in the PDMS membrane. In fact, the lower diffusion led to a stronger target-PDMS interaction, and the enrichment occurred inside the membrane. Moreover, PDMS also showed the hydrophobic interaction with the methyl and alkyls groups attached targets due to the Van der Walls force between the methyl group of PDMS and alkyl groups of targets [45]. As a consequence, one could assume that the toluene molecules were trapped by PDMS film efficiently, and it was believed that the PDMS film significantly improved the SERS detection sensitivity.

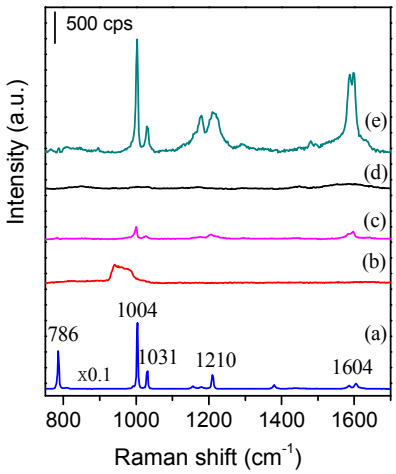

Figure 3 Normal Raman spectrum of toluene liquid (a); SERS spectra of toluene on PDMS coated Si wafer (b) and naked Au MLF (c). SERS spectrum from PDMS-Au MLF without (d) and with (e) toluene.

In order to further evaluate the performance of PDMS-Au MLF composite, the SERS detection on toluene with different concentrations from 5 mM down to 5 μM was performed on the PDMS-Au MLF composite (as shown in Figure 4). It can be found that, concomitantly with the decrease of the concentration of toluene solution, the SERS intensity of toluene decreased significantly both on naked Au MLF and PDMS-Au MLF substrate. By comparison, for the same concentration, the SERS intensity of toluene adsorbed on composite substrate was much higher than that adsorbed on naked Au MLF. For example, for the intensity of band at 1003 cm^{-1} in the 5 mM toluene solution, the SERS signal was about 9 times stronger than that from the naked Au MLF substrate. Furthermore, the SERS signal was negligible on the naked Au MLF as the concentration was less than 50 μM, while it was observed unambiguously from the composite substrate even though the concentration was downing to 5 μM (as shown in Figure 4b), and it was comparable to that observed from the 0.5 mM toluene adsorbed on naked Au MLF substrate. Therefore, by the spin coating of PDMS strategy, the limitation of detection (LOD) of SERS was improved with two orders of magnitude to achieve 5 μM (~0.5 ppm) for detecting the toluene in water.

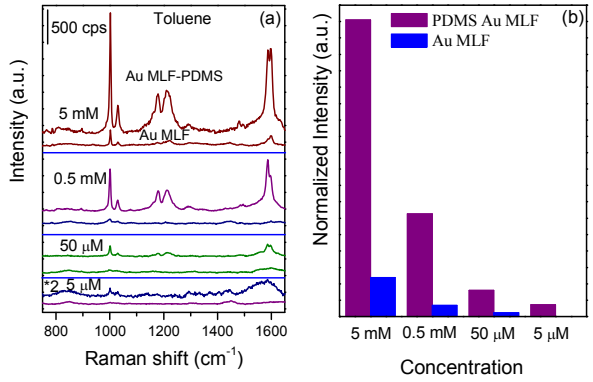

Figure 4 SERS spectra of toluene with different concentrations by using PDMS-Au MLF and Au MLF as substrates (a); the concentration dependent of SERS intensity of band at 1003 cm^{-1} (b).

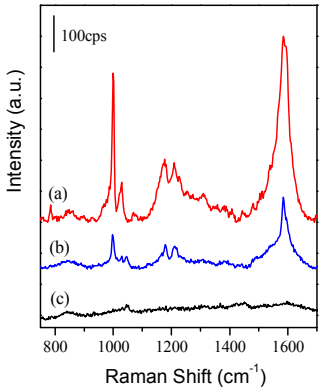

Figure 5 SERS spectra of toluene vapor detected by using PDMS-Au MLF (a), Au MLF (b) and blank PDMS Au MLF in atmospheres (c).

Detection of toluene gas in atmospheres

In fact, the VOC has been becoming the main pollutants in air, and thus the sensitive detection attracted considerable attention. Based on the fact that PDMS film exhibited the high efficiency for trapping aromatic molecules in water, it was worth to explore the performance of the PDMS-Au MLF composite in vapor detection. Due to the high vapor pressure of toluene, it was employed as model targets to evaluate the SERS capability for detecting toluene gas in the open atmosphere at room temperature. As described in the experimental section, the composition was located near the pure toluene liquids in the open atmosphere. With the volatilization of toluene at the open system, the target gas diffused around the toluene liquid and the PDMS Au MLF continuously captured the target gas molecule from the atmosphere. After reaching the maximum of SERS intensity, the SERS of toluene gas was subsequently recorded from the PDMS-Au MLF composition as presented in Figure 5 together with that from the naked Au MLF as comparison. Obviously, the SERS intensity from the former was about 5 times stronger than that from the latter, indicating the high performance of PDMS-Au MLF for detecting toluene gas. It demonstrated that the composite could be developed as the promising substrate to detect the small aromatic molecules both from aqueous and vapor phases with high sensitivity. Most importantly, this approach was also used to identify the targets by analyzing the fingerprint spectral information which was unique to each target.

Detection of benzene and nitrobenzene in water

As above mentioned, the PDMS hold the high performance for trapping the targets due to the interaction with PDMS film. Therefore, it was believed that the trapping capability for the weaker anchored targets should be decreased significantly, resulting the decreasing the sensitivity of SERS detection. In order to evaluate the generality of this strategy, the targets with the similar structure of toluene, involving benzene (about 23 mM for the saturated aqueous solution) and nitrobenzene (saturated concentration of 15.4 mM in water), were engaged as the model targets. [14, 44]

Figure 6 presented a series of SERS spectra of benzene with different concentrations adsorbed onto the PDMS-Au MLF and naked Au MLF substrates, respectively. The band at 994 cm^{-1} dominated in the SERS spectrum, which was assigned to the symmetric ring breathing, [42] while all of the other Raman bands were comparatively weak. It should be pointed, for the saturated benzene solution, the SERS intensity from the composite was about 7-8 times to that from the naked Au MLF substrate. The intensity decreased dramatically as the concentration was reduced from saturation to 1 mM, and it was almost disappeared on the Au MLF substrate for the 1 mM solution. However, for the PDMS-Au MLF composite substrate, the strongest SERS band of benzene could be distinguished in a 1mM solution, indicating the LOD was down about 5 times to 1 mM by comparing LOD of 5 mM for naked Au MLF substrate. Obviously, the LOD for benzene was higher at least two orders of magnitude than that of toluene by using the same SERS substrate. It indicated that the LOD of this approach was critically depended on the nature of targets. Since the Vander Waals forces between the methyl groups of the polymer and the methyl group of toluene, PDMS film offered the relative strong hydrophobic interaction with the toluene. Moreover, the diffusion coefficients illustrated the interaction between the PDMS and targets, the higher diffusion coefficient suggested the weaker interaction with the PDMS film. It was reported that the diffusion coefficient of toluene was smaller than that of benzene. [34, 44] Along with this line, the trapping capability of PDMS was dependent on the diffusion coefficient, and it was favorable for capturing toluene rather than benzene. In contrast with the diffusion coefficient, the permeability in PDMS film exhibited the opposite effect on the trapping capability for targets, i.e. the higher permeability represented the high performance of PDMS for capturing targets. However, the permeation process depended on both solubility and diffusion constants. Generally, permeability was higher for hydrophobic target compounds than polar ones, and it increased with the hydrophobicity. Mark et al. estimated the permeability of compounds in the sequence of: aromatic > alcohols, and 3C-benzenes >> 2C-benzenes. [44] Thus, the toluene permeated at a

greater extent than benzene through PDMS layer (about 2 times of benzene), which reduced the LOD remarkably. As a consequence, our present results were in well agreement with the previous literatures. [34,44] Furthermore, as the most rigorously detected targets, the LOD for benzene was about 1 mM (78 mg/L), i.e. about 78 ppm, which was comparable with that previous reported on a functionalized Au SERS substrate and was inferior to the thiol modified SERS substrate.[1, 15]

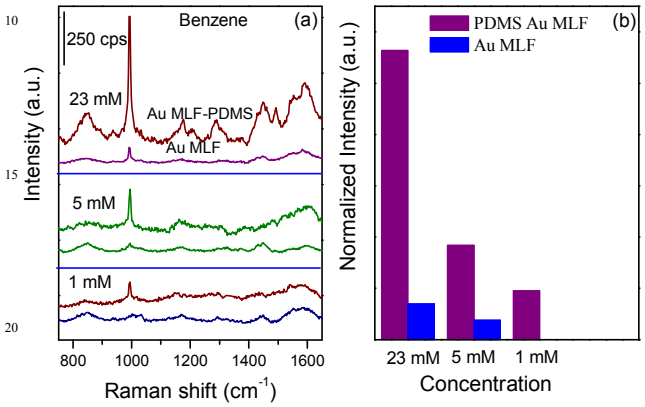

Figure 6 SERS spectra of benzene with different concentrations by using PDMS-Au MLF and Au MLF as substrates (a); the concentration dependent of SERS intensity of band at 994 cm^{-1} (b).

For another target, the characteristic Raman peaks of nitrobenzene could be divided two catalogues, including nitro group relevant and the ring relevant modes. The strongest SERS band at about 1343 cm^{-1} was assigned to symmetric stretching mode of nitro group, while the middle strong band at 1001 cm^{-1} was corresponding to ring breathing mode.[42] These bands were dominated in the SERS spectra presented in Figure 7.

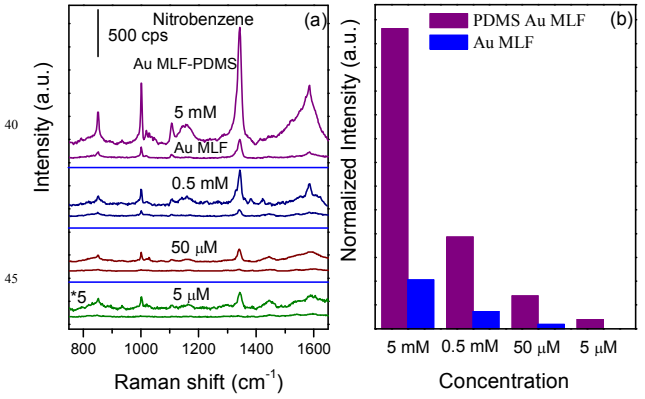

Figure 7 SERS spectra of nitrobenzene with different concentrations by using PDMS-Au MLF and Au MLF as substrates (a); the concentration dependent of SERS intensity of band at 1343 cm^{-1} (b).

By varying the concentration of nitrobenzene aqueous solution, it demonstrated that SERS signal of nitrobenzene from the naked Au MLF was relatively weaker than that from the PDMS-Au MLF composite substrate at same concentrations. As illustrated in Figure 7b, the LOD of SERS for nitrobenzene was about 5 μM and 0.5 mM on PDMS-Au MLF and naked Au MLF substrates, respectively. It should be pointed that the SERS signal of nitrobenzene with the concentration of 0.5 mM was almost negligible with a very low signal-to-noise on the naked Au MLF substrate (Figure 7b). Therefore, the comparable LOD was attributed to toluene and nitrobenzene, respectively. Actually, the hydrophobicity and permeability of nitrobenzene lied between the benzene and toluene, the low LOD was mainly contributed to the interaction of nitro group with Au surface, which increased the SERS signal remarkably. The higher permeability for toluene was served as the compensation against the very weak interaction with the Au surface. Nevertheless, the PDMS exhibited the stronger affinity for the methyl or nitro groups substituted aromatic molecules than that of benzene.

Conclusions

In summary, a facile strategy was developed to fabricate the PDMS-Au MLF composite substrate for the detection of aromatic molecules in water and atmosphere by SERS. The PDMS film was covered onto the Au MLF by the spin coating technique. By considering the influence on the SERS signal and the trapping capability, the concentration of PDMS base was1.25% to be used as the spin coating solution to reach the maximum SERS effect. The thickness of PDMS layer was about 129 nm to 139 nm.The PDMS-Au MLF composite held the higher capability than the naked Au MLF substrate for the targets in water or atmospheres. Moreover, the performance was dependent on the nature of the targets, i.e. the detection performance was in the sequence of toluene≈ nitrobenzene>benzene. The LOD was reached to 0.5 ppm, 78 ppm and 0.6 ppm for toluene, benzene and nitrobenzene, respectively. Although some issues, including the quantitative analysis and the identification on multi-targets, should be addressed, our results demonstrated that the present approach could be developed as a promising tool to detect numerous targets which were non-specifically adsorbed onto the metallic plasmonic nanostructures. It opened a window towards the general application in the in situ monitoring the pollutants in environmental science.

Acknowledgments

This work is supported by the National Nature Science Foundation of China (Nos. 21033007, 21173155, 21303115 and 21473118), the National Instrumentation Program (2011YQ031240402). The partial financial support from a Project Funded by the Priority Academic Program Development of Jiangsu Higher Education Institutions (PAPD). Natural Science Foundation of Jiangsu Province (BK2012187), the Natural Science Fundamental Research Project of Jiangsu Colleges and Universities (12KJD150011) is gratefully acknowledged.

Notes and references

[a] *College of Chemistry, Chemical Engineering and Materials Science, Soochow University, Suzhou, 215123, China.*
E-mail: yuanyaxian@suda.edu.cn, jlyao@suda.edu.cn

† Electronic Supplementary Information (ESI) available: [details of any supplementary information available should be included here]. See DOI: 10.1039/b000000x/

‡ Equal contribution

1 M. M. Loh, J. I. Levy, J. D. Spengler, E. A. Houseman and D. H. Bennett, *Environ. Health Persp.*, 2007, **115**, 1160-1168..

2 L. Molhave, G. Clausen, B. Berglund, J. De Ceaurriz, A. Kettrup, T. Lindvall, M. Maroni, A. C. Pickering, U. Risse, H. Rothweiler, B. Seifert and M. Younes, *Indoor Air*, 1997, **7**, 225-240.

3 S. Król, B. Zabiegała and J. Namieśnik, *Anal. Bioanal. Chem.*, 2011, **400**, 1751-1769..

4 L. C. Sander and S. A. Wise, *Anal. Chem.*, 1987, **59**, 2309-2313..

5 B. Sharma, R. R. Frontiera, A. I. Henry, E. Ringe and R. P. Van Duyne, *Mater.Today*, 2012, **15**, 16-25.

6 R. A. Alvarez-Puebla and L. M. Liz-Marzán, *Small*, 2010, **6**, 604-610.

7 C. L. Haynes, A. D. McFarland and R. P. Van Duyne, *Anal. Chem.*, 2005, **77**, 338 A-346 A.

8 A. Hakonen, M. Svedendahl, R. Ogier, Z.-J. Yang, K. Lodewijks, R. Verre, T. Shegai, P. O. Anderssonb and M. Käll, *Nanoscale*, 2015,**7**, 9405-9410.

9 A. Hakonen, P. O. Andersson, M. S. Schmidt, T. Rindzevicius and M. Kall, Anal. Chim. Acta., 2015 DOI:10.1016/j.aca.2015.04.010.

10 M. Moskovits, *Rev. Mod. Phys.*, 1985, **57**, 783-826.

11 K. A. Willets and R. P. Van Duyne, *Annu. Rev. Phys. Chem.*, 2007, **58**, 267-297.

12 A. Campion and P. Kambhampati, *Chem. Soc. Rev.*, 1998, **27**, 241-250.

13 D. W. Li, W. L. Zhai, Y. T. Li and Y. T. Long, *Microchim. Acta*, 2014, **181**, 23-43.

14 W. Hill, B. Wehling, C. G. Gibbs, C. D. Gutsche and D. Klockow, *Anal. Chem.*, 1995, **67**, 3187-3192.

15 C. Marenco, C. J. M. Stirling and J. Yarwood, *J. Raman Spectrosc.*, 2001, **32**, 183-194.

16 Y. F. Xie, X. Wang, X. X. Han, X. X. Xue, W. Ji, Z. H. Qi, J. Q. Liu, B. Zhao and Y. Ozaki, *Analyst*, 2010, **135**, 1389-1394.

17 I. Lopez-Tocon, J. C. Otero, J. F. Arenas, J. V. Garcia-Ramos and S. Sanchez-Cortes, *Anal. Chem.*, 2011, **83**, 2518-2525.

18 N. S. Myoung, H. K. Yoo and I. W. Hwang, *J. Nanophotonics*, 2014, **8**, 0830831-0830837.

19 C. L. Jones, K. C. Bantz and C. L. Haynes, *Anal. Bioanal. Chem.*, 2009, **394**, 303 -311.

20 L. G. Olson, R. H. Uibel and J. M. Harris, *Appl. Spectrosc.*, 2004, **58**, 1394 -1400.

21 J. J. Du and C. Y. Jing, *J. Phys. Chem. C*., 2011, **115**, 17829-17835.

22 Q. An, P. Zhang, J. M. Li, W. F. Ma, J. Guo, J. Hu and C. C. Wang, *Nanoscale*, 2012, **4**, 5210-5216.

23 Z. Y. Bao, X. Liu, Y. Chen, Y. C. Wu, H. L. W. Chan , J. Y. Dai and D. Y. Lei, *J. Hazard. Mater*., 2014, **280**,706-712.

24 L. E. Kreno, N. G. Greenelth, O. K. Farha, J. T. Hupp and R. P. Van Duyne, *Analyst*, 2014, **139**,4073-4080.

25 K. Sugikawa, Y. Furukawa and K. Sada, *Chem. Mater*, 2011, **23**, 3132-3134.

26 D. Y. Siberio-Pérez, A. G. Wong-Foy, O. M. Yaghi and A. J. Matzger, *Chem. Mater*, 2007, **19**,3681-3685.

27 Y. L. Hu, J. Liao, D. M. Wang and G. K. Li, *Anal. Chem.*, 2014, **86**, 3955-3963.

28 K. S. Giesfeldt, R. M. Connatser, M. A. De Jesús, P. Dutta and M. J. Sepaniak , *J. Raman Spectrosc.*, 2005, **36**, 1134-1142

29 J. Olavarría-Fullerton, S. Wells, W. Ortiz-Rivera, M. J. Sepaniak and M. A. De Jesus, *Appl. Spectrosc.*, 2011, **65**, 423-428.

30 M. A. De Jesus, K. S. Giesfeldt and M. J. Sepaniak, *Appl. Spectrosc.,* 2004, **58**, 1157-1164.

31 M. Wang, B. De Vivo, W. J. Lu and M. Muniz-Miranda, *Appl. Spectrosc.*, 2014, **68**, 784-788.

32 R. Gupta and G. U. Kulkarni, *ChemSusChem*, 2011, **4**, 737-743.

33 M. Lamotte, P. F. De Violet, P. Garrigues and M. Hardy, *Anal. Bioanal. Chem*. 2002, **372**, 169-173.

34 K. P. Chao, V. S. Wang, H. W.Yang and C. I. Wang, *Polym. Test.*, 2011, **30**, 501-508.

35 S. Seethapathy and T. Górecki , *Anal. Chim. Acta*, 2012, **750**, 48-62.

36 G. Frens, *Nature. Phys. Sci.*, 1973, **241**, 20-22.

37 L. Scarabelli, M. Coronado-Puchau, J. J. Giner-Casares, J. Langer and L. M. Liz-Marzan , *ACS Nano*, 2014, **8**, 5833-5842.

38 M. Bračič, T. Mohan, R. Kargl, T. Griesser, S. Hribernik, S. Köstler, K. Stana-Kleinschek and L. Fras-Zemljič, *RSC. Adv*., 2014, **4**, 11955-11961.

39 J. H. Koschwanez, R. H. Carlson and D. R. Meldrum, *PLoS one*, 2009, **4**, e4572.

40 T. Shahal, K. A. Melzeak, C. R. Lowe and E. Gizeli, *Langmuir*, 2008, **24**, 11268- 11275.

41 P. Gao and M. J. Weaver, *J. Phys. Chem*, 1985, **89**, 5040-5046.

42 P. Gao and M. J. Weaver, *J. Phys. Chem.*, 1989, **93**, 6205-6211.

43 D. L. Stokes, A. Pal, V. A. Narayanan and T. vo-Dinh, *Anal. Chim. Acta.*, 1999**, 399**, 265-274.

44 E. Boscaini, M. L. Alexander, P. Prazeller and T. D. Mark, *Int. J. Mass spectrom*., 2004, **239**, 179-186.

45 I. Arslan-Alaton and J. L. Ferry, *Appl. Catal. B-Environ.*, 2002, **38**, 283-293.